Interaction of Gangliosides with Proteins Depending on Oligosaccharide Chain and Protein Surface Modification

Mitsuhiro Hirai, Hiroki Iwase, Shigeki Arai, Toshiharu Takizawa, and Kouhei Hayashi
Department of Physics, Gunma University, Maebashi 371, Japan

ABSTRACT By using neutron and synchrotron x-ray small-angle scattering techniques, we investigated the process of the complexation of gangliosides with proteins. We treated monosialoganglioside (G_{M1}), disialoganglioside (G_{D1a}), and a mixture of G_{M1}/G_{D1a}. Proteins used were bovine serum albumins whose surfaces were modified with different sugars (deoxy-D-galactose, deoxy-L-fucose, deoxymaltitol, and deoxycellobiitol), which were used as model glycoproteins in a membrane. We found that the complexation of gangliosides with albumins greatly depends on the combination of ganglioside species and protein surface modification. With a varying protein/ganglioside ratio in a buffer solution at pH 7, the complexation of G_{M1} or G_{D1a} with albumins modified by monosaccharides appears to be less destructive for ganglioside aggregate structures in forming large complexes; the complexation of G_{D1a} with the albumins modified by disaccharides induces the formation of complexes with a dimeric structure; and the complexation of G_{M1} with albumins modified by disaccharides, to form small complexes, is very destructive. The present results show a strong dependence of the interaction between ganglioside and protein on the characteristics of the ganglioside and protein surface, which would relate to a physiological function of gangliosides, such as a function regulating the receptor activity of glycoproteins in a cell membrane.

INTRODUCTION

Gangliosides, the most complex of the glycosphingolipids, are most abundant in the plasma membrane of nerve cells (making up 5–10% of the total lipid mass) and are found widely in most vertebrate cell types (Mikata and Taniguchi, 1985). Gangliosides are acidic glycolipids composed of a ceramide linked to an oligosaccharide chain containing one or more *N*-acetylneuraminic acid (called sialic acid) residues. Through the study of the great variety of structures of the oligosaccharide chains, gangliosides have been clarified to play an important role in various physiological surface events such as cell differentiation, transmembrane signaling, regulation of cell growth, and so on (Hansson et al., 1977; Hakomori, 1986; Spiegel and Fishman, 1987; Hannun and Bell, 1989; Hakomori and Igarashi, 1993; Svennerholm et al., 1994). Such physiological functions are closely related to the physicochemical properties of ganglioside molecules, which have been studied intensively. The presence of large hydrophilic headgroups of ganglioside molecules has been shown to lead to a marked amphiphilic property and a micellar aggregation in aqueous solutions, rather than to vesicles or bilayers (Ulrich-Bott and Wiegandt, 1984; Tettamanti et al., 1985; Corti and Cantù, 1990; Sonnino et al., 1994).

To clarify the physicochemical mechanism of the appearance of physiological functions of gangliosides, we have been studying, by scattering techniques and calorimetry, the functional structures of gangliosides in aqueous dispersions in connection with thermotropic phase behaviors and hydrodynamic properties (Hirai et al., 1997). Previously one of our authors (Hayashi and Katagiri, 1974) found an interesting phenomenon in the interaction of gangliosides with proteins, that is, the solubility of gangliosides to biphasic solvent (the upper hydrophilic phase and the lower hydrophobic phase) changes drastically with the addition of methylated bovine albumin, which was used as a model chemical of basic proteins in synaptic membranes. Recently we showed that this phenomenon results from the heterogeneous (patchlike) binding of gangliosides to an albumin molecule and from the oligomeric lipoprotein formation depending on protein concentration (Hirai et al., 1995a; Takizawa et al., 1995). Those results suggested that interactions of gangliosides with proteins depend on protein surface structures. In the present study, by using x-ray and neutron scattering techniques, we found evident differences in the complexation processes of three different types of ganglioside samples with various bovine serum albumins whose surfaces were chemically modified with different saccharides, where these chemically modified albumins were used as model glycoproteins in a membrane.

MATERIALS AND METHODS

Sample preparation

Three different types of gangliosides from bovine brain were purchased from Sigma Chemical Co.: monosialoganglioside (Galβ1–3GalNAcβ1–4(NeuAcα2–3)Galβ1–4Glcβ1–1Cer, abbreviated as G_{M1}); disialoganglioside (NeuAcα2–3Galβ1–3GalNAcβ1–4(NeuAcα2–3)Galβ1–4Glcβ1–1Cer, abbreviated as G_{D1a}); and type III (containing 20% sialic acid) (Gammack, 1963). The purity was monitored by thin-layer chromatography (TLC). The G_{M1} or G_{D1a} sample gave a single spot on a TLC plate. The major components of the type III sample were G_{M1} and G_{D1a} gangliosides in equimolar amounts. The lipidic portion (ceramide) of the natural ganglioside extracted from bovine brain was shown to be formed

Received for publication 22 April 1997 and in final form 28 November 1997.

Address reprint requests to Dr. Mitsuhiro Hirai, Department of Physics, Gunma University, 4–2 Aramaki, Maebashi 371, Japan. Tel.: +81-272-20-7554; Fax: +81-272-20-7551; E-mail: hirai@sun.aramaki.gunma-u.ac.jp.

0006-3495/98/03/1380/08 $2.00

primarily by a long-chain fatty acid (stearic acid, which makes up 90% or more of the total fatty acid content) and a long-chain base (C18 and C20 unsaturated sphingosine, which is generally more than 10% of the total content) (Sonnino et al., 1986). We prepared buffer solvents: 0.01 M citrate buffer in H_2O adjusted at pH 6.7; 50 mM HEPES buffer at pH 7.0 in H_2O for the x-ray scattering experiments; and 50 mM HEPES buffer at pH 7.0 in 100%, 60%, 41%, and 0% (v/v) D_2O/H_2O for the neutron scattering experiments. Four different types of bovine serum albumins whose molecular surfaces were chemically modified with different saccharides were purchased from Sigma Chemical Co.: albumin−2-amido-2-deoxy-D-galactose, albumin−1-amido-1-deoxy-L-fucose, albumin-*N*-1-[deoxymaltitol], and albumin-*N*-1-[deoxycellobiitol] were used as model glycoproteins. Methyl ester of bovine albumin was used as a control protein without sugars. By using sodium dodecyl sulfate-polyacrylamide gel electrophoresis, we checked the purity of each albumin sample to show a single band. In the following sections we use abbreviations to designate the above albumins (gal-, fuc-, mal-, cel- and met-albumins, respectively). The albumin stock solutions were prepared by dissolving the albumins into the above buffer solvents with different concentrations. The ganglioside stock solutions were also prepared by dissolving gangliosides in the buffer solvents. The concentrations of the ganglioside stock solutions were 1.0% (w/v) for x-ray scattering experiments and 2.0% (w/v) for neutron scattering experiments. The samples for the scattering measurements were prepared by mixing equal volumes of the above ganglioside and albumin stock solutions. The final concentrations of gangliosides were 0.5% (w/v) for x-ray scattering samples and 1.0% (w/v) for neutron scattering samples.

Scattering experiments

Small-angle x-ray scattering experiments were carried out by using the synchrotron radiation small-angle x-ray scattering spectrometer installed at the synchrotron source (PF) at the National Laboratory for High-Energy Physics (KEK), Tsukuba, Japan (Ueki et al., 1985). The wavelength used and the covered q range were 1.49 Å and 0.01–0.25 $Å^{-1}$, respectively, where q is the magnitude of scattering vector defined by $q = (4\pi/\lambda)\sin(\theta/2)$ (θ is the scattering angle; λ is the wavelength). The sample-to-detector distance was 88 cm. The sample was contained in a sample cell with a pair of mica windows. The sample cell was placed in a cell holder kept at 25°C. The exposure time of one measurement was 300 s. Neutron scattering experiments were done by using the small-/medium-angle neutron diffractometer installed at the pulsed neutron source at KEK. As this spectrometer uses a white pulsed neutron beam of 1–16 Å wavelength based on the time-of-flight method, it can cover a very wide q range of 0.015–5 $Å^{-1}$ in one measurement. The detail of the spectrometer was reported elsewhere (Furusaka et al., 1992). In the neutron scattering experiments, a solvent contrast variation method was employed (Stuhrmann and Miller, 1978). The exposure time of one sample was varied from 1 h to 6 h, depending on the D_2O/H_2O ratio of the solvent.

Scattering data analysis

After data corrections, the following analyses were carried out according to standard methods. The distance distribution function $p(r)$ was calculated by the Fourier inversion of the scattering intensity $I(q)$ as

$$p(r) = \frac{2}{\pi}\int_0^\infty rqI(q)\sin(rq)\mathrm{d}q \tag{1}$$

The $p(r)$ function reflects the particle shape, the intraparticle scattering density distribution, and the interparticle correlation (Glatter, 1982). The maximum dimension D_{max} of the particle is estimated from the $p(r)$ function satisfying the condition $p(r) = 0$ for $r > D_{max}$. During the calculation of the $p(r)$ function, the extrapolation of the small-angle data sets by use of the Guinier plot ($\ln(I(q))$ versus q^2) and modification of the scattering intensity as

$$I'(q) = I(q)\exp(-kq^2) \tag{2}$$

(k is the artificial damping factor) were employed to reduce the Fourier truncation effect.

To estimate a gyration radius R_g and a total scattering intensity I_{total}, we used the following equations (Glatter, 1982), where I_{total} and R_g are given by

$$I_{total} = \int_0^{D_{max}} p(r)\mathrm{d}r \tag{3}$$

and

$$R_g^2 = \frac{\int_0^{D_{max}} p(r)r^2\mathrm{d}r}{2\int_0^{D_{max}} p(r)\mathrm{d}r} \tag{4}$$

Equation 3 was used for normalization of the $p(r)$ functions.

As shown previously (Hirai et al., 1993), the scattering function of a complex composed of structural subunits that have simple geometrical shapes can be calculated by using the following equation:

$$I(q) \propto (4\pi)^{-1}\int_\Omega \sum_{i=1}^{n}\sum_{j=1}^{n} A_i(q)A_j^*(q)\exp\{iq\cdot(r_i - r_j)\}\mathrm{d}\Omega \tag{5}$$

where $A_i(q)$ is the structure factor of the ith subunit with the mass center coordinate r_i. Here we have simplified the shapes of subunits to spheres, ellipsoids, or cylinders.

RESULTS

Complexation of G_{M1} and G_{D1a} gangliosides with albumins

Figs. 1 and 2 show the x-ray scattering curves $I(q)$ depending on the albumin/G_{M1} ganglioside ratio and on the albumin/G_{D1a} ganglioside ratio, where *A*, *B*, and *C* correspond to the additions of gal-, fuc- and mal-albumins, respectively. The scattering curves of the G_{M1} and G_{D1a} suspensions without albumins in Figs. 1 and 2 show a saturating tendency of the scattering intensity below $q \approx 0.04$ $Å^{-1}$ and have an evident minimum at $q \approx 0.06–0.07$ $Å^{-1}$, followed by a rounded peak at $q \approx 0.09–0.11$ $Å^{-1}$. This suggests that both G_{M1} and G_{D1a} ganglioside suspensions are highly monodispersed and consist of globular particles (namely micelles), because a polydispersity of solute particles in shape or dimension strongly smears the scattering curve. As the albumins are added to the ganglioside suspensions, the scattering curves vary and lose their initial characteristics. Below the albumin/ganglioside ratios of 1/1 for G_{M1} and 1.25/1 for G_{D1a}, the additions of gal- and fuc-albumins induce a gradual change in the scattering curves by shifting the minimum and rounded peak positions, which are almost smeared above the ratios of 2/1 and 2.5/1. The fast increasing tendencies of the scattering intensities below $q \approx 0.04$ $Å^{-1}$ show that the complexation of gangliosides with albumins induces the formation of polydispersed large aggregates, except for the case of the complexation of the G_{M1}

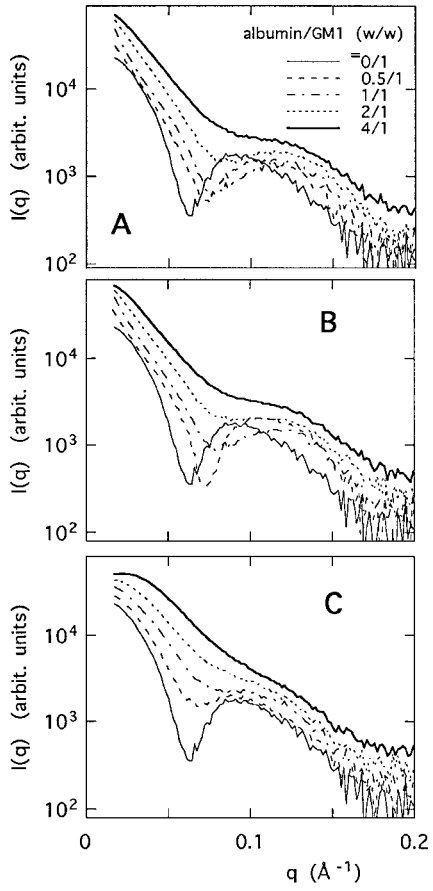

FIGURE 1 X-ray scattering curves $I(q)$ of albumin/G_{M1} ganglioside mixture suspensions in 0.01 M citrate buffer at pH 6.7 at 25°C. The ganglioside concentrations were 0.5% w/v, and the albumin concentrations were varied from 0 to 2.0% w/v. Three different types of albumins were used: (*A*) albumin−2-amido-2-deoxy-D-galactose; (*B*) albumin−1-amido-1-deoxy-L-fucose; (*C*) albumin-*N*-1-[deoxymaltitol].

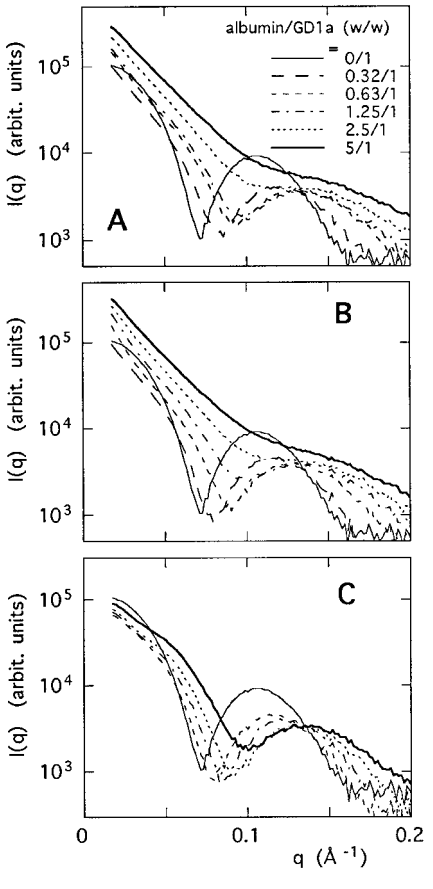

FIGURE 2 X-ray scattering curves $I(q)$ of albumin/G_{D1a} ganglioside mixture suspensions in 0.01 M citrate buffer at pH 6.7 at 25°C. The ganglioside concentrations were 0.5% w/v, and the albumin concentrations were varied from 0 to 2.5% w/v. Three different types of albumins were used. *A*, *B*, and *C* are as in Fig. 1.

gangliosides with mal-albumins. On the addition of mal-albumins, the scattering curves of the G_{M1} and G_{D1a} suspensions change in a manner that is very different from the above cases. Thus, in the case of G_{D1a}, the scattering curve shows a minimum and a rounded peak, even at the highest albumin/ganglioside ratio, despite the addition of mal-albumins; in contrast, the addition of mal-albumins greatly affects the scattering curve of the G_{M1} suspension from the lowest albumin/ganglioside ratio of 0.5/1.

Figs. 3 and 4 show the distance distribution functions $p(r)$ obtained by the Fourier inversion; Eq. 1 was used for the scattering curves in Figs. 1 and 2. Determined structural parameters are shown in Table 1. The $p(r)$ profiles of the G_{M1} and G_{D1a} suspensions without albumins are characterized by a shoulder of ~25–40 Å and a peak of ~71–76 Å, suggesting the presence of scattering objects, with a strong fluctuation of the intraparticle scattering density distribution, namely ganglioside micelles. Such a $p(r)$ profile apparently reflects the intramicellar structure, which is composed of a hydrophobic moiety (ceramides) and of a hydrophilic moiety (oligosaccharide chains with sialic acids). By x-ray analysis, these different moieties have large negative and positive excess scattering densities (so-called contrasts), respectively, compared to the average scattering density of water solvent. The maximum dimension D_{max} of the micelle estimated from the $p(r)$ function satisfying the condition $p(r) = 0$ for $r > D_{max}$ is 130 ± 1 Å for G_{M1} and 111 ± 1 Å for G_{D1a}. The gyration radius R_g estimated by Glatter's method and using Eq. 4 is 51.9 ± 0.4 Å for G_{M1} and 44.4 ± 0.3 Å for G_{D1a}. In the cases of the additions of gal- and fuc-albumins to the G_{M1} and G_{D1a} suspensions, the $p(r)$ profiles show the low humps around 140–150 Å below the albumin/ganglioside ratios of 1.25/1 for G_{M1} and of 1/1 for G_{D1a}, and these humps become to be smeared at high albumin concentrations. In the case of the addition of mal-albumins to the G_{D1a} suspension, the presence of the hump becomes to be much clearer at the highest albumin concentration. Various types of complexes are known to show different $p(r)$ profiles (Hirai et al., 1993); thus the appearance of these humps is attributable to the presence of complexes with dimeric or dumbbell structures in face-to-face contact as a major component (Glatter, 1982; Matsushita et al., 1989), which is shown in the following modeling

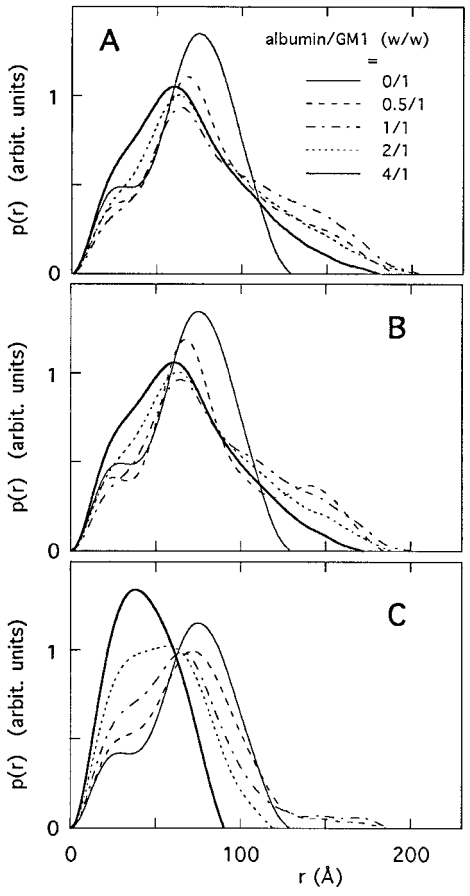

FIGURE 3 Distance distribution functions $p(r)$ of albumin/G_{M1} ganglioside mixture suspensions calculated by the Fourier inversion of the scattering curves $I(q)$ in Fig. 1. *A*, *B*, and *C* are as in Fig. 1.

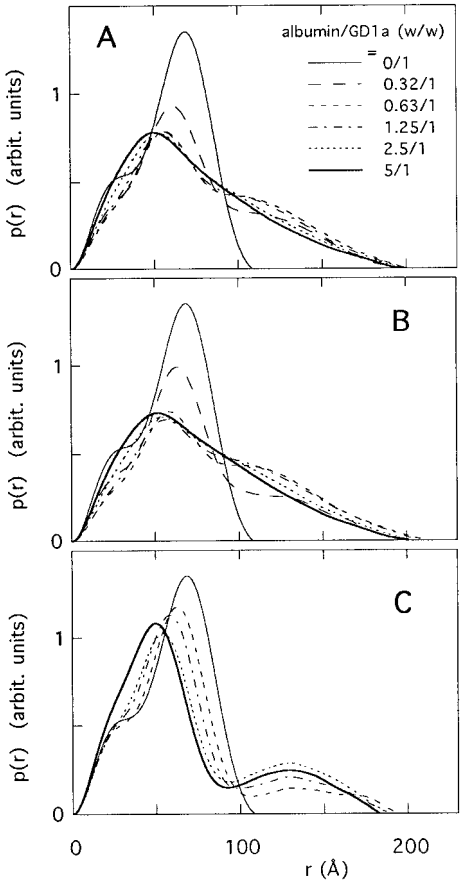

FIGURE 4 Distance distribution functions $p(r)$ of albumin/G_{D1a} ganglioside mixture suspensions calculated by the Fourier inversion of the scattering curves $I(q)$ in Fig. 2. *A*, *B*, and *C* are as in Fig. 2.

analyses. In contrast to the above case, the addition of mal-albumins to the G_{M1} suspension significantly changes the $p(r)$ profile, especially at the highest protein concentration to show a single bell-shaped peak with a small D_{max} value, which indicates the presence of monodispersed small globular particles. Thus the interaction between G_{M1} gangliosides and mal-albumins can be assumed to be strong enough to destroy the initial structure of the ganglioside aggregates compared with other cases.

In Fig. 5 the protein concentration dependence of the R_g values estimated by Glatter's method is shown, which well reflects the above changing tendencies. In the cases of the addition of gal- and fuc-albumins, the R_g value increases significantly below the albumin/ganglioside ratio of ~1/1, and gradually decreases with increasing albumin concentrations. In the case of the addition of mal-albumins, the R_g value gradually increases for G_{D1a}, and, in contrast, decreases monotonously for G_{M1} with increasing protein concentration.

Modeling analyses

As discussed in the above section, the $p(r)$ profile of the complex of G_{D1a} with mal-albumins at high protein concentration suggests the presence of dimeric or dumbbell structures in face-to-face contact. By using Eq. 5, we can tentatively simulate various types of dimeric particles; the $p(r)$ functions of two different types of model dimeric particles are shown in Fig. 6. These model structures were searched mostly to reproduce the experimental $p(r)$ profile, namely, the D_{max} value and the positions of the peak and the hump. For model B, the simple dimer composed of spheres with a radius of 46 Å was assumed. For model C, a dumbbell particle composed of two spheres (40 Å in radius and with relative contrast of 1) and one cylinder (20 Å in radius, 40 Å in height, and a relative contrast of 0.6) was assumed. Model A represents a sphere 20 Å in radius, which gives the experimental R_g value of mal-albumin. The ratio of the

TABLE 1 Structural parameters of ganglioside micelles (G_{M1} and G_{D1a}) at 25°C at pH 7.0 for G_{M1} and at pH 6.7 for G_{D1a}

	R_{q^a} (Å)	R_{q^b} (Å)	p_{max} (Å)	D_{max} (Å)
[G_{M1}]	47.7 ± 1.8	51.9 ± 0.4	76 ± 1	130 ± 1
[G_{D1a}]	44.6 ± 0.8	44.4 ± 0.3	71 ± 1	111 ± 1

The ganglioside concentration was 0.5% (w/v). R_{g^a} and R_{g^b}, the gyration radii estimated by the Guinier approximation and Glatter's method, respectively.

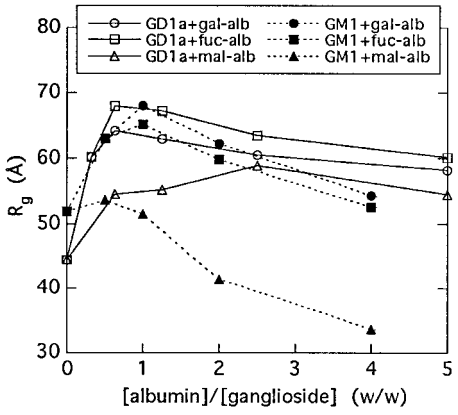

FIGURE 5 Variation of gyration radii R_g of albumin/ganglioside mixture suspensions depending on protein concentrations. Open and full marks correspond to albumin/G_{D1a} and albumin/G_{M1} mixtures, respectively. ○ and ●, Albumin^{-2}-amido-2-deoxy-D-galactose; □ and ■, albumin^{-1}-amido-1-deoxy-L-fucose; △ and ▲, albumin-*N*-1-[deoxymaltitol]. R_g values were determined by using Glatter's method in Figs. 3 and 4.

relative contrast values of the sphere and cylinder for model C was assumed to correspond to the ratio of the absolute contrast values of the protein and ganglioside molecules. As shown by model D in Fig. 6, the more appropriate $p(r)$ function was obtained by the mixture of the dumbbell particles and the small spheres. If various types of complexes with different shapes and dimensions had coexisted in equal amounts, the $I(q)$ and $p(r)$ would have given very smeared profiles. The model presented in Fig. 6 would greatly simplify the present solution system; however, we

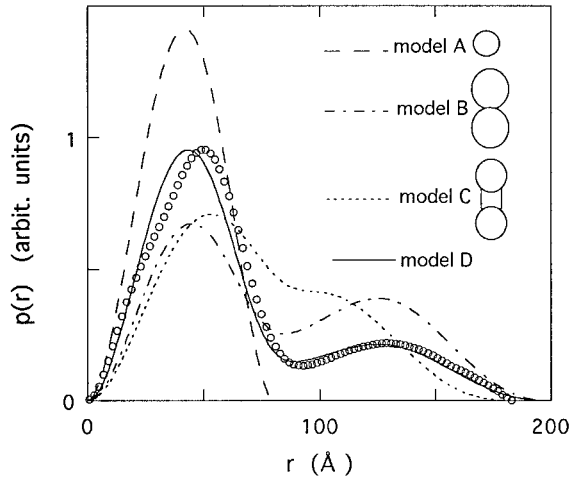

FIGURE 6 Model $p(r)$ functions for the complex of G_{D1a} with mal-albumins at high protein concentration. Model A sphere with radius of 20 Å; model B, dimmer composed of spheres with radius of 46 Å; model C, dumbbell particle composed of two spheres (40 Å in radius and relative contrast of 1) and one cylinder (20 Å in radius, 40 Å in height, and relative contrast of 0.6); model D, mixture of model A and model C. The $p(r)$ functions are normalized by the total scattering intensity I_{total}. ○, Experimental $p(r)$ function of the mal-albumin/G_{D1a} ganglioside = 5/1 (w/w) mixture solution in Fig. 4 *C*.

can assume the presence of complexes with a dimeric or dumbbell shape as a major component.

Complexation of type III gangliosides with albumins measured by neutron scattering

As shown in Fig. 7, by using the solvent contrast variation method, we measured the scattering curves of the type III gangliosides solubilized in 100%, 60%, 41%, and 0% (v/v) D_2O/H_2O HEPES buffers, and determined the contrast matching point to be ~25% (v/v) D_2O/H_2O. To compare with the previous results on the interaction of crude mixture (G_M/G_D) with met-albumin, we focused the present neutron scattering experiments to observe the complexation of the ganglioside mixture (G_{M1}/G_{D1a}) with albumin at low protein concentrations, below the albumin/ganglioside ratio of 0.5/1, by using 41% (v/v) D_2O/H_2O solvent. This value mostly agrees with that obtained in our previous study (Hirai et al., 1995b). Then the scattering curve only reflected the change of the ganglioside aggregate structure, because the 41% (v/v) D_2O/H_2O solvent is the contrast matching point of albumin (Hirai et al., 1995a). Fig. 8 shows the neutron scattering curves $I(q)$ depending on the albumin/type-III ganglioside ratio, where *A*, *B*, and *C* correspond to the complexation of the gangliosides with gal-, cel- and met-albumins, respectively. The difference of the effect of the additions of the above albumins on the ganglioside aggregate structures is clearly recognized in Fig. 8. Thus the albumin modified by monosaccharides (gal-albumin) hardly affects the aggregate structure below the albumin/ganglioside ratio of 0.25/1; the albumin modified by disaccharides (cel-albumin) gradually changes the aggregate structure with increasing protein concentration; and the albumin without saccharides (met-albumin) drastically changes the aggregate structure even at the lowest protein concentration, which agrees with our previous results (Hirai et al., 1995a). Fig. 9 shows the scattering curves obtained by the synchrotron radiation x-ray scattering for the same sam-

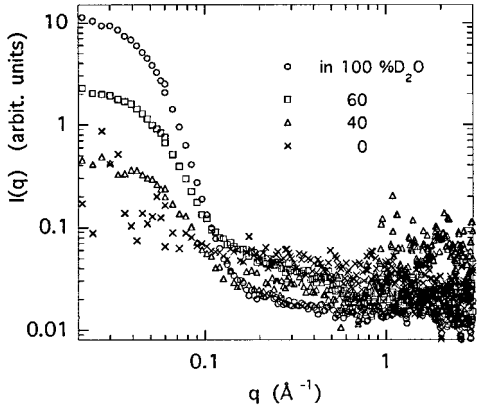

FIGURE 7 Solvent contrast dependence of neutron scattering curve $I(q)$ of type III gangliosides in 50 mM HEPES buffer at pH 7.0 at 25°C. ○, □, △, ×, Solutions in 100%, 60%, 40%, and 0% (v/v) D_2O/H_2O buffer solvents, respectively.

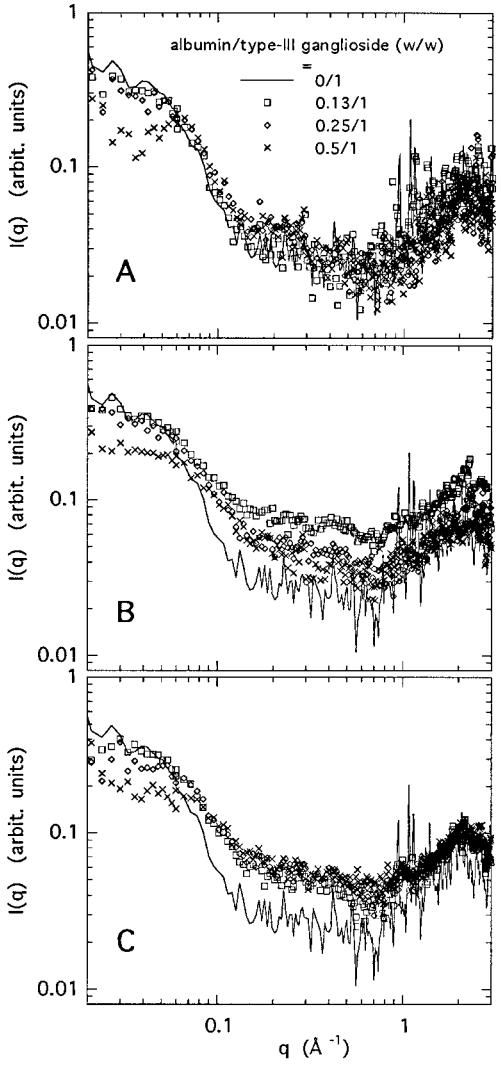

FIGURE 8 Neutron scattering curves $I(q)$ of albumin/type III ganglioside mixture suspensions in 50 mM HEPES buffer (41% v/v, D_2O/H_2O) at pH 7.0 at 25°C. Forty-one percent (v/v) D_2O/H_2O is the contrast matching point of albumin. The ganglioside concentration was 1.0% (w/v), and the albumin concentration was varied from 0 to 0.5% (w/v). Three different types of albumins were used: (*A*) albumin^{-2}-amido-2-deoxy-D-galactose; (*B*) albumin-*N*-1-[deoxycellobiitol]; (*C*) methyl ester of bovine albumin.

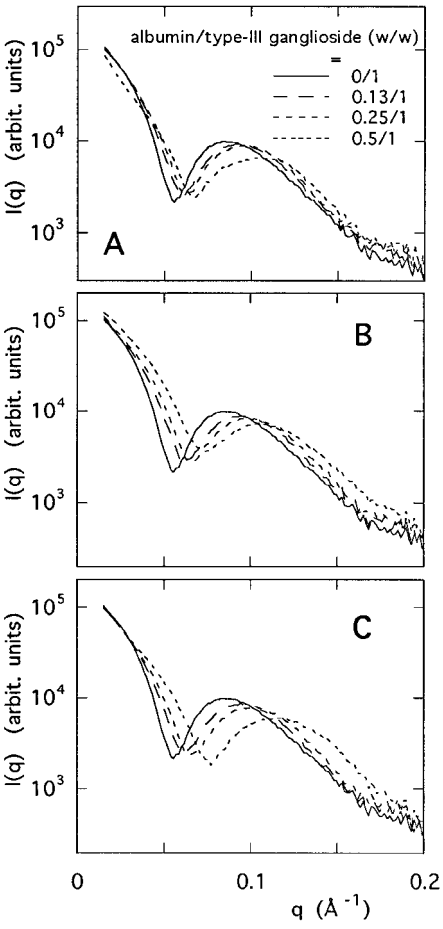

FIGURE 9 X-ray scattering curves $I(q)$ of albumin/type III ganglioside mixture suspensions in 50 mM HEPES buffer (41% v/v, D_2O/H_2O) at pH 7.0 at 25°C. The samples were as same as those used for the neutron scattering experiments in Fig. 7. *A*, *B*, and *C* are as in Fig. 7.

ples used for the neutron scattering experiments. Although the x-ray scattering data reflect the change of the whole structure of the complex, in Fig. 9 we can recognize the difference in the complexation process of gangliosides with different proteins, namely that the addition of cel-albumins induces a more evident change of the scattering curve from the lowest protein concentration in comparison with the case of the addition of gal-albumins, which resembles the case of the addition of met-albumins. These changing tendencies agree with the above results obtained from the neutron scattering measurements. Both neutron and x-ray scattering results evidently show the difference in the binding affinities of gangliosides with albumins, depending on protein surface modifications.

DISCUSSION

The results from the x-ray scattering experiments indicate that the interaction between gangliosides and albumins greatly depends both on species of gangliosides and on surface modifications of albumins. The complexation processes of G_{M1} and G_{D1a} gangliosides with the albumins modified by monosaccharides show a similar tendency, which appears to be less destructive for ganglioside aggregate structures and the formation of polydisperse large complexes. On the other hand, the complexation of G_{M1} or G_{D1a} gangliosides with albumins modified by disaccharides occurs in a manner different from that of the above cases. That is, the complexation of G_{D1a} gangliosides with albumins modified by disaccharides induces the formation of complexes with a dimeric or dumbbell structure, and in the case of G_{M1} gangliosides the complexation appears to be very destructive for ganglioside aggregate structures, suggesting a strong interaction between G_{M1} gangliosides and albumins modified by disaccharides. The results from neutron scattering experiments strongly support the above x-ray scattering results, and demonstrate the binding affinity of

gangliosides with albumins, depending on the protein surface modification. Combined with both x-ray and neutron scattering results, we can assume the following. The interaction of G_{M1} gangliosides with an albumin modified by monosaccharides and the interaction of G_{D1a} gangliosides with an albumin modified by mono- or disaccharides proceed at the interfacial area of the protein surface to form oligomeric complexes. On the other hand, the interaction between G_{M1} gangliosides with an albumin modified by disaccharides promotes monomeric complex formation, destroying ganglioside aggregate structures.

As we have shown recently (Hirai et al., 1997), both factors, namely the flexibility of the oligosaccharide chain of ganglioside molecules and the interaction between oligosaccharide chains, are essentially important to determining the stability of the ganglioside aggregate structure. A recent NMR study also suggests the intrinsic dynamic structural properties of the oligosaccharide chain affecting the geometrical properties of the aggregates (Acquotti et al., 1994). Such intrinsic structural properties of gangliosides that depend on oligosaccharide chains would be involved in a variety of interactions with other ligands. Interactions of gangliosides with various ligands have been studied intensively by many investigators using various methods. Although the x-ray and neutron scattering methods do not afford us a high-resolution crystallographic picture of the complex, as shown for the complex of G_{M1} with cholera toxin B-pentamer (Merritt et al., 1997), by the complementary use of x-ray and neutron scattering techniques, we have partly understood the characteristics of the interaction of gangliosides with a glycoprotein through saccharide residues, which greatly depend both on the oligosaccharide chain of the ganglioside and on the protein surface. Another recent study has clearly indicated, by using electron microscopy, the presence of a ganglioside molecule-enriched plasma membrane domain (Sorice et al., 1997), which would support some biological meaning of the present experimental systems, treating interaction between ganglioside micelle and protein as a model system for studying the interaction between the ganglioside-enriched domain and ligands. Although the present results do not show directly a specific binding affinity of gangliosides for a glycoprotein in a membrane, the present results would relate to some biological function of gangliosides, such as a function regulating the well-known receptor activity of glycoproteins on a cell membrane (Allaway and Burness, 1986; Paul and Lee, 1987), through the great variety of the oligosaccharide chains of ganglioside molecules.

This work was done under the approval of the Photon Factory Program Advisory Committee of the National Laboratory for High-Energy Physics (proposals 93G047, 95G084, and 96G157). This work was financially supported by a Grant-in-Aid for Scientific Research from the Ministry of Education, Science and Culture of Japan (08680712).

REFERENCES

Acquotti, D., L. Cantu, E. Ragg, and S. Sonnino. 1994. Geometrical and conformational properties of ganglioside GalNAc-G_{D1a}, $IV^4GalNAcIV^3Neu5AcII^3Neu5AcGgOse_4Cer$. *Eur. J. Biochem.* 225: 271–288.

Allaway, G. P., and A. T. H. Burness. 1986. Site of attachment of encephalomyocarditis virus on human erythrocytes. *J. Virol.* 59: 768–770.

Corti, M., and L. Cantù. 1990. Application of scattering techniques in the domain of amphiphiles. *Adv. Colloid Interface Sci.* 32:151–166.

Furusaka, M., K. Suzuya, N. Watanabe, M. Osawa, I. Fujikawa, and S. Satoh. 1992. WINK (small-/medium-angle diffractometer). *KEK Prog. Rep.* 92–2:25–27.

Gammack, D. B. 1963. Physicochemical properties of ox-brain gangliosides. *Biochem. J.* 88:373–383.

Glatter, O. 1982. Data treatment. *In* Small Angle X-ray Scattering. O. Glatter and O. Kratky, editors. Academic Press, London. 119–196.

Hakomori, S. 1986. Glycosphingolipids. *Sci. Am.* 254:32–41.

Hakomori, S., and Y. Igarashi. 1993. Gangliosides and glycosphingolipids as modulators of cell growth, adhesion, and transmembrane signaling. *Adv. Lipid Res.* 25:147–162.

Hannun, Y. A., and R. M. Bell. 1989. Functions of sphingolipids and sphingolipid breakdown products in cellular regulation. *Science.* 243: 500–507.

Hansson, H. A., J. Holmgren, and L. Svennerholm. 1977. Ultrastructural localization of cell membrane GM1 ganglioside by cholera toxin. *Proc. Natl. Acad. Sci. USA.* 74:141–145.

Hayashi, K., and A. Katagiri. 1974. Studies on the interaction between gangliosides, protein and divalent cations. *Biochim. Biophys. Acta.* 337: 107–117.

Hirai, M., S. Arai, H. Iwase, S. Yabuki, T. Takizawa, and K. Hayashi. 1998. Characteristics of thermotropic phase transition of glycosphingolipid (ganglioside) aggregates in aqueous solution. *Thermochim. Acta.* 308:93–99.

Hirai, M., R. Kawai-Hirai, T. Hirai, and T. Ueki. 1993. Structural change of jack bean urease induced by addition of surfactants studied with synchrotron-radiation small-angle x-ray scattering. *Eur. J. Biochem.* 215:55–61.

Hirai, M., T. Takizawa, S. Yabuki, Y. Nakata, H. Mitomo, T. Hirai, S. Shimizu, M. Furusaka, K. Kobayashi, and K. Hayashi. 1995a. Complexes of gangliosides with proteins in solution. *Physica B.* 213, 214: 751–753.

Hirai, M., S. Yabuki, T. Takizawa, Y. Nakata, H. Mitomo, T. Hirai, S. Shimizu, K. Kobayashi, M. Furusaka, and K. Hayashi. 1995b. Ganglioside structure in solution. *Physica B.* 213, 214:748–750.

Matsushita, N., Y. Izumi, T. Matsuo, H. Yoshino, T. Ueki, and Y. Miyake. 1989. Binding of both Ca^{2+} and mastoparan to calmodulin induces a large change in the tertiary structure. *J. Biochem.* 105:883–887.

Merritt, E. A., S. Sarfaty, M. G. Jobling, T. Chang, R. K. Holmes, T. R. Hirst, and W. G. Hol. 1997. Structural studies of receptor binding by cholera toxin mutants. *Protein Sci.* 6:1516–1528.

Mikata, A., and N. Taniguchi. 1985. Glycosphingolipid. *In* Glycolipids. H. Weigandt, editor. Elsevier, New York. 59–82.

Paul, R. W., and P. W. K. Lee. 1987. Glycophorin is the reovirus receptor on human erythrocytes. *Virology.* 159:94–101.

Sonnino, S., D. Acquotti, L. Riboni, A. Giuliani, G. Kirschner, and G. Tettamanti. 1986. New chemical trends in ganglioside research. *Chem. Phys. Lipids.* 42:3–26.

Sonnino, S., L. Cantù, M. Corti, D. Acquotti, and B. Venerando. 1994. Aggregative properties of gangliosides in solution. *Chem. Phys. Lipids.* 71:21–45.

Sorice, M., I. Parolini, T. Sansolini, T. Garofalo, V. Dolo, M. Sargiacomo, T. Tai, C. Peschle, M. R. Torrisi, and A. Pavan. 1997. Evidence for the existence of ganglioside-enriched plasma membrane domains in human peripheral lymphocytes. *J. Lipid Res.* 38:969–980.

Spiegel, S., and P. H. Fishman. 1987. Gangliosides as bimodal regulators of cell growth. *Proc. Natl. Acad. Sci. USA.* 84:141–145.

Stuhrmann, H. B., and A. Miller. 1978. Small-angle scattering of biological structures. *J. Appl. Cryst.* 11:325–345.

Svennerholm, L., A. K. Asbury, R. A. Reisfeld, K. Sandhoff, K. Suzuki, G. Tettamanti, and G. Toffano. 1994. Biological Function of Gangliosides. Elsevier, Amsterdam.

Takizawa, T., M. Hirai, S. Yabuki, Y. Nakata, A. Takahashi, and K. Hayashi. 1995. Calorimetric, small-angle x-ray, and neutron scattering studies of mixing ganglioside and methylated albumin. *Thermochim. Acta.* 267:355–364.

Tettamanti, G., S. Sonnion, R. Ghidoni, M. Masserini, and B. Venerando. 1985. Chemical and functional properties of gangliosides. Their possible implication in membrane-mediated transfer of information. *In* Physics of Amphiphiles: Micelles, Vesicles, and Microemulsions. M. Corti and V. Degiorgio, editors. North-Holland, Amsterdam. 607–636.

Ueki, T., Y. Hiragi, M. Kataoka, Y. Inoko, Y. Amemiya, Y. Izumi, H. Tagawa, and Y. Muroga. 1985. Aggregation of bovine serum albumin upon cleavage of its disulfide bonds, studied by the time-resolved small-angle x-ray scattering technique, with synchrotron radiation. *Biophys. Chem.* 23:115–124.

Ulrich-Bott, B., and H. Wiegandt. 1984. Micellar properties of glycosphingolipids in aqueous media. *J. Lipid Res.* 25:1233–1245.